

## Soliton Experiments in Stimulated Raman Scattering<sup>1</sup>

R. G. Wenzel, J. L. Carlsten, and K. J. Drühl

---

Experimental observations of solitons in stimulated Raman scattering are reported. Soliton formation resulted from the introduction of a  $\pi$  phase shift in the incident Stokes beam as predicted by theory. Pulse sharpening and retardation on propagation in the Raman medium have been observed along with amplitude diminution. The first two features were predicted and the third was not. Spontaneous soliton formation has been observed in the absence of any amplitude modulation or apparent phase shift in the optical fields, indicating that additional sets of initial conditions may result in soliton formation.

---

**KEY WORDS:** Soliton; stimulated Raman scattering.

Although it has been known since the mid-1970's that the equations of stimulated Raman scattering (SRS) admit soliton solutions in the hypertransient limit,<sup>(1-8)</sup> the only observations of solitons is SRS at present have been in highly transient scattering of CO<sub>2</sub> laser radiation from gaseous H<sub>2</sub>. Indeed, it now appears that medium transiency provides a mechanism whereby disturbances occurring on the same time scale as the coherent decay may be temporally sharpened on propagation through the medium and thus become hypertransient.<sup>(9)</sup> The observations to follow should therefore be thought of as pertaining to solitons in an early stage of evolution.

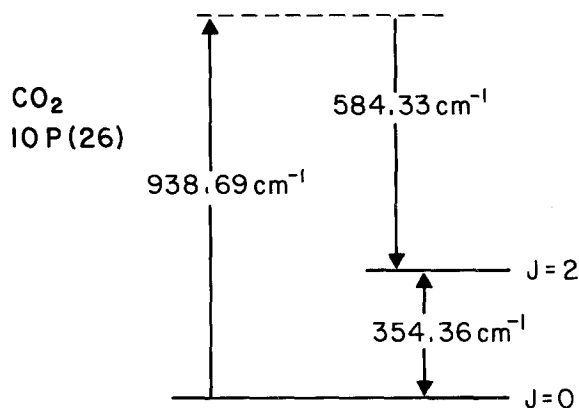
The initial observations of soliton formation were made during studies of down-conversion of 10- $\mu$ m pump radiation to 16  $\mu$ m via SRS from the  $S_0(0)$  transition in para-H<sub>2</sub>.<sup>(10)</sup> Figure 1 shows the energy level diagram and the experimental apparatus used is shown in Fig. 2. The CO<sub>2</sub> pump laser oscillator contains a low-pressure gain cell and apertures in order to

---

<sup>1</sup> Work performed under the auspices of the U.S. Department of Energy.

<sup>2</sup> Chemistry Division, Los Alamos National Laboratory, Los Alamos, New Mexico 87545.

<sup>3</sup> Institute for Modern Optics, University of New Mexico, Albuquerque, New Mexico 87131.



### para-H<sub>2</sub>

Fig. 1. Energy level diagram of frequencies involved in a typical Raman scattering experiment.

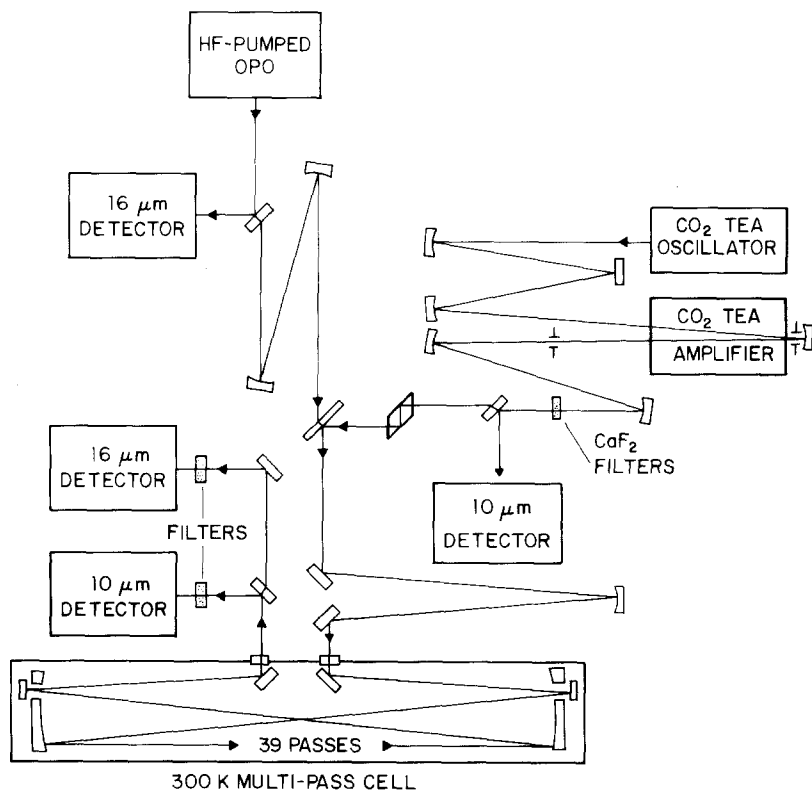


Fig. 2. Schematic of the basic experimental setup.

limit oscillation to a single longitudinal and transverse mode. The amplifier increases the energy to about 2 J and a Fresnel rhomb circularly polarizes the beam for maximum Raman gain. An input Stokes beam is added to the pump on a dichroic reflector and the two beams are mode matched into a multipass cell (MPC) containing 1 atm of para- $\text{H}_2$ . The temporal pulse shapes of the output pump and Stokes beams are observed on photon drag detectors.

The CdSe optical parametric oscillator (OPO) which provides the input Stokes pulse at  $16\ \mu\text{m}$  is pumped with the  $P_2(7)$  line of an HF laser at  $2.9\ \mu\text{m}$ . Because CdSe exhibits absorption at  $16\ \mu\text{m}$ , the cavity is designed to oscillate at  $3.5\ \mu\text{m}$ , which corresponds to a difference frequency of  $8.6 \times 10^{13}$  Hz between the  $2.9\text{-}\mu\text{m}$  pump and the  $16\text{-}\mu\text{m}$  output. The  $2.9\text{-}\mu\text{m}$  pump laser has a bandwidth  $< 5 \times 10^{-4}\ \text{cm}^{-1}$ , and therefore narrowing the resonant  $3.5\text{-}\mu\text{m}$  field narrows the  $16\text{-}\mu\text{m}$  output. However, any frequency or phase shift in either the resonant or the pump field results in a

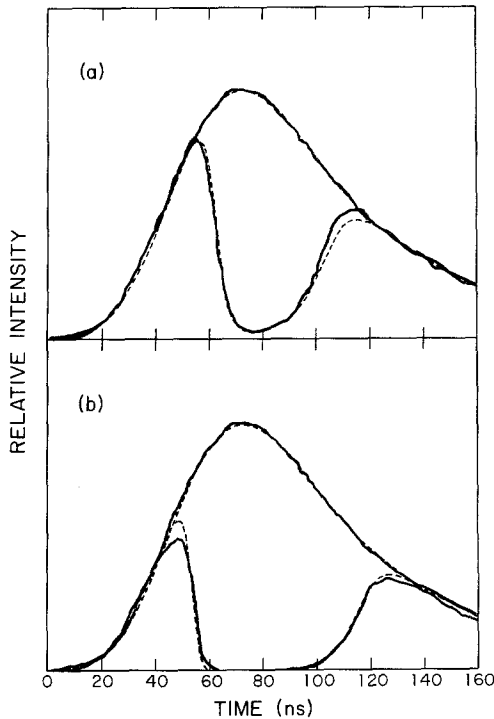


Fig. 3. Pulse shapes of the incident and depleted pump in "normal" pump depletion. The incident pump power was 5.5 MW in (a) and 7.6 MW in (b). Solid lines are the experimental shapes and the dashed lines are the theoretical fit (from Ref. 11).

comparable shift in the 16- $\mu\text{m}$  output. The 2.9- $\mu\text{m}$  pump pulse shape is frequently found to exhibit mode beating when observed with a fast detector, suggesting the possibility of mode competition and hopping. It is thought that pump laser mode hopping is the source of input Stokes phase shifts which result in the spontaneous formation of solitons in SRS.

Figure 3 shows the conversion profiles obtained in normal pump depletion at two levels of  $\text{CO}_2$  pump intensity. For simplicity, the output Stokes pulse shape is not included in Fig. 3, but has been observed to be the difference between the input and output  $\text{CO}_2$  pump pulses. Note that the intensity at which depletion begins is considerably greater than that at which it ends, a direct result of transiency. The coherence decay time of the

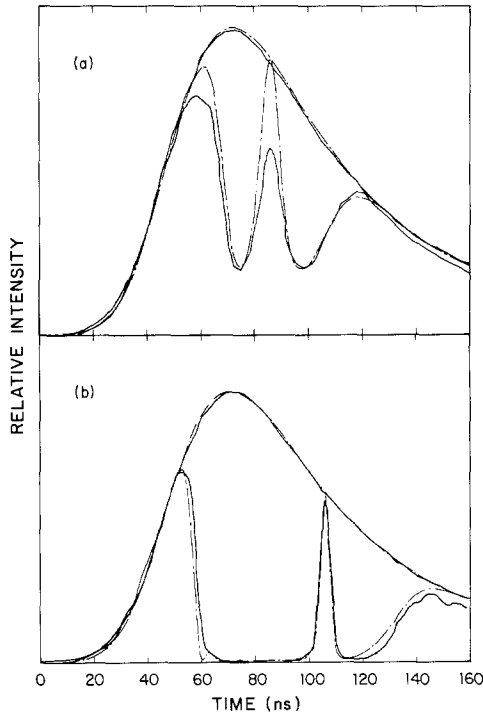


Fig. 4. (a) Comparison of experimental and theoretical pulse shapes of the incident and depleted pump pulse showing anomalous reversal of pump depletion which we interpret as the development of a solution induced by a random phase shift in the injected OPO Stokes beam. Solid lines are the experimental shapes and the dot-dashed lines are the theoretical fit. The theoretical curve was generated by introducing a  $\pi$  phase shift in the Stokes beam at 71 nsec. The incident pump power was  $\sim 5$  MW. (b) Another example similar to that in (a) but with the pump power raised to  $\sim 7$  MW. Note that the generated pulse has shortened considerably because of the higher gain. In this case the theoretical curve was generated by introducing a  $\pi$  phase shift in the Stokes beam at 81 nsec.

$S_0(0)$  transition is about 3 nsec at a pressure of 1 atm. The 3-nsec decay time plays a strong role in the formation of pulse shapes measured in several tens of nanoseconds because of the very large gain. The dashed curves represent theoretical calculations including coherence decay.<sup>(11)</sup>

Figure 4 shows typical examples of the spontaneous depletion reversal which is observed to occur randomly with a frequency of perhaps 1 in 20. While complete reversals (in which the peak goes all the way back to the undepleted envelope) are common, partial reversals are more frequently seen. Narrower pulses are invariably seen at higher Raman gain. The dashed curves result from calculations using the same model as that of Fig. 3 with a  $\pi$  phase shift introduced in the input Stokes beam. These calculations predict a narrowing at greater gain. The analytical soliton solutions of the SRS hypertransient equations also admit partial reversals (resulting from detuning from Raman resonance) and a propagation

### SEQUENTIAL RAMAN AMPLIFIERS

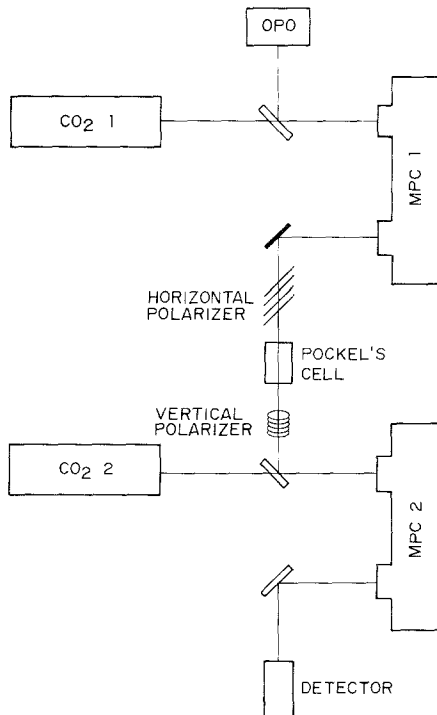


Fig. 5. Sequential Raman amplifiers used in first attempt to generate solitons in SRS by the introduction of a  $\pi$  phase shift in the input Stokes beam.

velocity less than the velocity of light. Indeed, in the calculations represented in Fig. 4, the phase shift times were variable parameters and the best fits to the data were obtained for shifts at 14 and 21 nsec prior to the observed reversals in retarded time in the two cases shown. Thus, explanations for two of the observed features (narrowing and partial reversal) are suggested and a third ( $v < c$ ) is predicted by theory.

Initial experiments to induce soliton formation were performed on apparatus shown schematically in Fig. 5. The Stokes output from the first MPC is separated from the depleted pump and passed through a Pockel's cell between crossed polarizers. Application of two voltage pulses of opposite polarity to the Pockel's cell results in the transmission of two Stokes pulses out of phase with one another by  $\pi$  radians as shown in Fig. 6. The voltage pulses are adjusted so as to minimize the time between

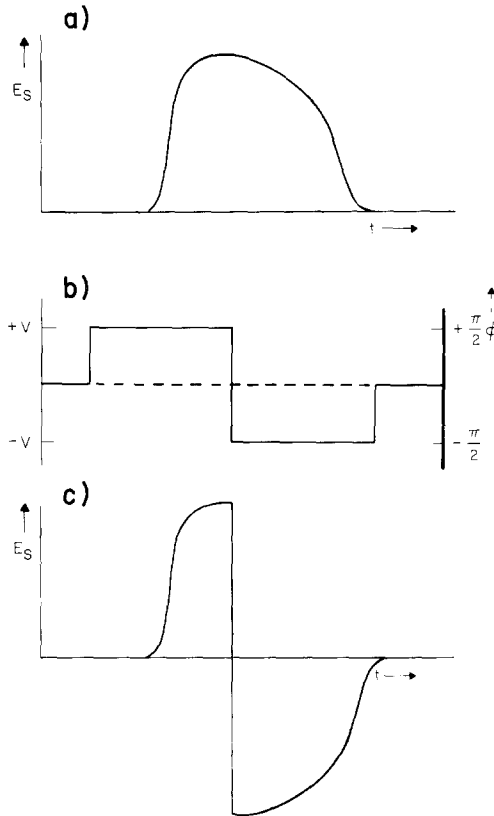


Fig. 6. Introduction of the  $\pi$  phase shift. (a) Output Stokes amplitude from first Raman cell; (b) voltage pulse applied to Pockel's cell and phase shift introduced in transmitted pulse; (c) Stokes amplitude input to second Raman cell.

the two transmitted pulses. The Stokes pulse containing the phase shift thus produced was combined with a pump pulse from a second  $\text{CO}_2$  laser and the two were injected into a second MPC identical to the first.

Production of solitons in this system was highly erratic and appeared to be associated with fine tuning of the cavity length of the second  $\text{CO}_2$  laser. As the free spectral range of each of the  $\text{CO}_2$  cavities used is 100 MHz it seems reasonable to suppose that lack of mode beating implies that a mode within  $\sim 30$  MHz of line center is oscillating for each laser. Thus the Stokes output of the first MPC should be resonant in the second within the Raman bandwidth of 51 MHz.<sup>(12)</sup> The apparent sensitivity of soliton formation to detuning from Raman resonance is not understood at this time.

A modification to the apparatus to reduce detuning uncertainty is shown in Fig. 7. Since both of the  $\text{CO}_2$  amplifiers are driven from the same

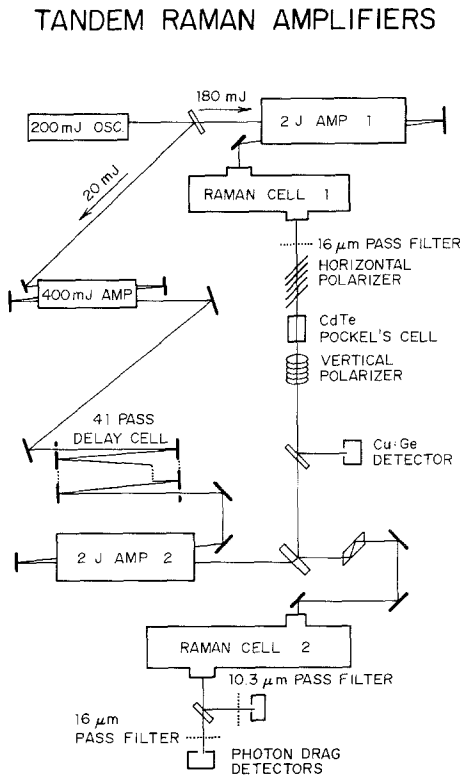


Fig. 7. Tandem Raman amplifiers producing Stokes and pump pulses in resonance with the  $S_0(0)$  transition.

single mode oscillator, the two pump lasers are expected to have the same frequency to within the transform limit of 3.5 MHz. The transit times through the two legs of the system are the same to within 2 nsec. The Stokes transmitted by the Pockel's cell and the pump output of the second MPC were monitored on detectors which were synchronized in retarded time. Typical results are shown in Fig. 8. The notch in the Stokes pulse indicates the time of the  $\pi$  phase shift and the 13-nsec delay of the reversal agrees with theory within experimental error. Solitons were observed to form each time the phase shift was induced in the Stokes beam. Their amplitude, however, was highly variable.

In recent experiments, spontaneous solitons from one Raman cell have been injected into a second cell (the pump beam was not separated from the Stokes, nor were any phase shifts nor additional pump pulses introduced). In this way it was possible to examine solitons at two points in a Raman medium. A typical result is shown in Fig. 9. Narrowing of the pulse and a 5-nsec delay are directly observed. Of greater interest is a diminution of reversal. On examination of a number of events, such diminution is commonly seen and appears related to failure to achieve full reversal early in the formation process.

An analysis of the behavior of the phase of the pulse transmitted by a Pockel's cell including leakage through the polarizers suggests an explanation for the incomplete reversal and the amplitude diminution. It is shown in Appendix I that the phase of the leakage component is

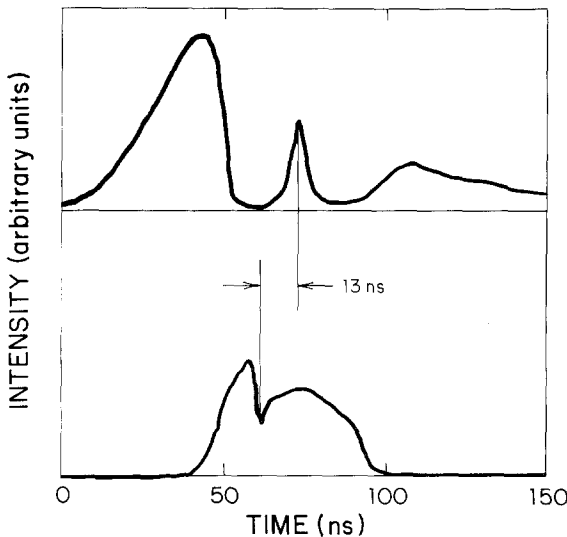


Fig. 8. Lower: Input Stokes pulse to Raman cell. Upper: Output pump pulse.



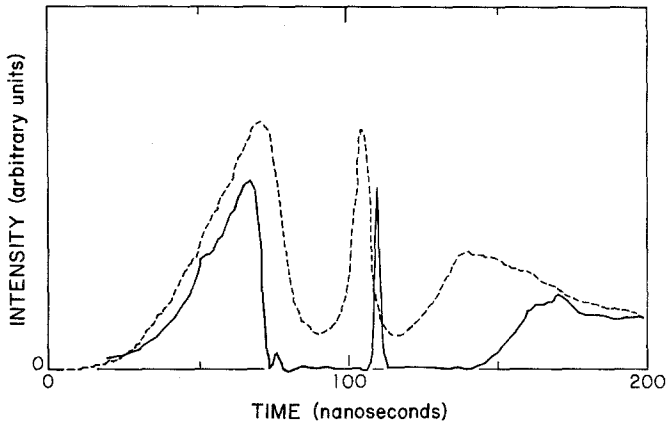


Fig. 9. Dashed curve: Pump pulse containing soliton introduced into Raman cell. Solid curve: Soliton exiting from Raman cell, showing narrowing and retardation. Note amplitude diminution.

unchanged when voltage is applied to the cell. Recent calculations<sup>(13)</sup> show that for a 1% leakage the reversal is typically 80% complete while for a 10% leakage the reversal is  $\sim 28\%$  complete. The reversal is also dependent on the rate of change of the phase. Furthermore, the reversal is found to decay as the disturbance propagates through the Raman medium. While this is not a complete explanation of the highly variable amplitudes, it gives some insight into the behavior of incomplete disturbances and their decay. The dynamics of soliton formation is an area of considerable interest and activity both theoretically and experimentally.

In addition to the solitons already described, spontaneous solitons have also been observed under other initial conditions. In particular, in continuing studies of the effects of transiency on Raman conversion, numerous experiments have been performed in which the Stokes output from one Raman cell is used as the input Stokes to a second cell, with no induced phase shift provided (such Stokes input pulses are superior to those provided by an OPO because they are more nearly in Raman resonance, they have well-behaved smooth envelope functions, are nearly Gaussian in spatial profile, and have high intensity). Such pulses are monitored before entering the MPC to ensure that they contain no solitons. The pump pulses are also monitored for mode beating. However, on rare occasions there are solitons in the output even when the input Stokes and pump pulse appear to be well behaved.

For experiments in Raman conversion outside the wavelength range of the OPO, it is possible to amplify spontaneous emission up to a useful level (including pump depletion). In one such experiment the MPC's were

adjusted for 55 passes to increase the interaction length and filled with normal hydrogen to make the  $S_0(1)$  ortho- $H_2$  transition ( $587.04\text{ cm}^{-1}$ ) available. The pump lasers were adjusted to oscillate on the  $9R(12)$  line of  $CO_2$  ( $1073.28\text{ cm}^{-1}$ ). Stokes output pulses at  $20.6\text{-}\mu\text{m}$  were produced with energies up to 100 mJ. Solitons were seen, once again on rare occasions, in these pulses generated from spontaneous emission. Considerable work remains to be done to discover all of the initial conditions which may result in soliton formation.

In conclusion, we have observed pump depletion reversal in SRS of beams from a  $CO_2$  laser operating at several frequencies from the  $S_0(0)$  and  $S_0(1)$  transitions in gaseous  $H_2$  which have been interpreted as solitons. Excellent fits to the experimental data have been obtained from transient theoretical calculations of pulse shapes resulting from phase shifts in the input Stokes beam. Soliton formation has been observed in the laboratory when phase shifts have been induced in the input Stokes beam, and the observed delay is in agreement with theory. Solitons have also been observed at two positions during propagation through the Raman medium, directly confirming pulse retardation and sharpening predicted by theory. Theoretical calculations based on incomplete polarization of the Stokes input beam suggest a mechanism for incomplete reversal other than detuning from resonance. These calculations also predict the diminution of reversal when incomplete, as observed experimentally.

Finally, solitons have been seen to form spontaneously in the apparent absence of phase shifts in either the pump or Stokes beams, indicating that additional sets of initial conditions may result in soliton formation in SRS.

## APPENDIX

### The phase and amplitude of a light wave transmitted by a Pockel's cell between crossed polarizers with leakage.

A circularly polarized wave incident upon the first polarizer may be written

$$E_0 = Ee^{i\phi}(\mathbf{i} + i\mathbf{j})$$

where  $\mathbf{i}$  and  $\mathbf{j}$  are unit vectors in the horizontal and vertical directions, respectively. If the first polarizer has unit transmission in the horizontal direction and (amplitude) transmission  $t$  in the vertical direction, the wave incident upon the Pockel's cell becomes

$$E_1 = Ee^{i\phi}(\mathbf{i} + it\mathbf{j})$$

The voltage is applied to the CdTe crystal of the Pockel's cell along the (110) direction, which is vertical in this work. Thus the major axis of

the induced index ellipsoid is at  $45^\circ$  to the vertical.<sup>(14)</sup> We choose  $\mathbf{i}'$  and  $\mathbf{j}'$  to be unit vectors along the induced major and minor axes:

$$\mathbf{i} = \frac{1}{\sqrt{2}}(\mathbf{i}' - \mathbf{j}')$$

$$\mathbf{j} = \frac{1}{\sqrt{2}}(\mathbf{i}' + \mathbf{j}')$$

Then

$$\mathbf{E}_1 = \frac{1}{\sqrt{2}} E e^{i\phi} [(1 + it)\mathbf{i}' - (1 - it)\mathbf{j}']$$

When a voltage is applied to the crystal, the component along  $\mathbf{i}'$  is shifted by  $\theta$ , while that along  $\mathbf{j}'$  is shifted by  $-\theta$ . Thus the wave transmitted by the crystal is

$$\mathbf{E}_2^{+V} = \frac{1}{\sqrt{2}} E e^{i\phi} [(1 + it)e^{i\theta}\mathbf{i}' - (1 - it)e^{-i\theta}\mathbf{j}']$$

On reversal of the voltage we have

$$\mathbf{E}_2^{-V} = \frac{1}{\sqrt{2}} E e^{i\phi} [(1 + it)e^{-i\theta}\mathbf{i}' - (1 - it)e^{i\theta}\mathbf{j}']$$

In terms of  $\mathbf{i}$  and  $\mathbf{j}$

$$\mathbf{E}_2^{+V} = E e^{i\theta} [(\cos \theta - t \sin \theta)\mathbf{i} + i(\sin \theta + t \cos \theta)\mathbf{j}]$$

$$\mathbf{E}_2^{-V} = E e^{i\phi} [(\cos \theta + t \sin \theta)\mathbf{i} - i(\sin \theta - t \cos \theta)\mathbf{j}]$$

The second polarizer will have unit transmission in the vertical direction and transmission  $t$  in the horizontal. The transmitted waves through this element become

$$\mathbf{E}_3^{+V} = E e^{i\phi} [i \sin \theta \mathbf{j} + t \cos \theta (\mathbf{i} + i\mathbf{j})]$$

$$\mathbf{E}_3^{-V} = E e^{i\phi} [-i \sin \theta \mathbf{j} + t \cos \theta (\mathbf{i} + i\mathbf{j})]$$

where terms in  $t^2$  have been dropped. The main part of the vertically polarized component is seen to be shifted by  $\pi/2$  during the  $+V$  pulse and  $-\pi/2$  during the  $-V$  pulse, while the leakage remains circularly polarized and is unshifted.

## REFERENCES

1. F. Y. F. Chu and A. C. Scott, *Phys. Rev. A* **12**:2060 (1975).
2. N. Tan-no, T. Shirahata, K. Yokoto, and H. Inaba, *Phys. Rev. A* **12**:159 (1975).
3. F. Y. F. Chu, in *Backland Transformations*, R. M. Miura, ed., Lecture Notes in Mathematics, No. 515 (Springer, New York, 1976).
4. M. K. Konopnicki and J. H. Eberly, *Phys. Rev. A* **24**:2567 (1981).
5. C. R. Stroud and D. A. Cardimona, *Opt. Commun.* **37**:221 (1981).
6. D. J. Kaup, *Physica* **6D**:143 (1983).
7. H. Steudel, *Physica* **6D**:155 (1983).
8. R. Meinel, *Opt. Commun.* **49**:224 (1984).
9. K. J. Drühl, J. L. Carlsten, and R. G. Wenzel, *J. Stat. Phys.* **39**:615 (1985), in this issue.
10. K. Drühl, R. G. Wenzel, and J. L. Carlsten, *Phys. Rev. Lett.* **51**:1171 (1983).
11. J. L. Carlsten, R. G. Wenzel, and K. Drühl, in *Proceedings of the Los Alamos Conference on Optics '83, Proc. Soc. Photo-Opt. Inst. Eng.* **380** (1983).
12. R. A. J. Keijser, J. R. Lombardi, K. D. Van den Hout, B. C. Sanctuary, and H. F. P. Knaap, *Physica* **76**:585 (1974).
13. J. Ackerhalt, private communication.
14. S. Namba, *J. Opt. Soc. Am.* **31**:76 (1961).